

Günay Çifçi · Derman Dondurur · Mustafa Ergün

Deep and shallow structures of large pockmarks in the Turkish shelf, Eastern Black Sea

Received: 1 February 2003 / Accepted: 27 August 2003 / Published online: 16 October 2003
© Springer-Verlag 2003

Abstract Circular and elongated pockmarks are present between 180- and 300-m water depths in the Eastern Black Sea shelf. The circular pockmarks have diameters of 50–120 m and the elongated pockmarks are 150–200 m wide with crater depths of 10–25 m. In deeper sediments, buried pockmarks were ‘vertically stacked’, indicating that the pockmarks developed under periodically varying overpressure conditions driven by the seismologically active North Anatolian Fault. Linear elongated pockmarks were formed by downslope tensional stretching, which caused linear weak zones together with strong seafloor currents acting as a connector of circular pockmarks.

Introduction

Shallow gas accumulations in seafloor sediments have been recognized on echo-sounder and side-scan sonar records by acoustic anomalies since the 1950s (Schüller 1952). The evidence for shallow gas accumulations in shallow marine sediments has been provided by high-resolution seismic and sub-bottom profiling techniques. The most common gas is methane, even though different kinds of gases may be produced in marine sediments. Methane is usually generated by the natural decomposition of organic matter—microbial gas generation—in shallow marine sediments. Shallow gas accumulations can be formed in bays and estuaries (Acosta 1984; Hovland and Judd 1988; Fader 1991; Garcia-Garcia et al. 1999), and in major deltas (Milliman and Butenko 1985; Hart and Hamilton 1993). Çifçi et al. (2002) and

Ergün et al. (2002) reported that large amounts of microbial methane production, accumulation, and expulsion took place at the Turkish shelf of the Eastern Black Sea.

Due to continuous sediment loading and tectonic compression, gas generated in near-surface sediments and pore fluids becomes overpressured and migrates to the seafloor via permeable pathways (e.g., Yun et al. 1999). These pathways can be faults, stratigraphic layers (Orange et al. 2002), mud diapirs (Hovland and Curzi 1989; Moore et al. 1991) or the pathways formed by migrating gas in porous sediments, for example, clays, silts and muds (Judd and Sim 1998; Harrington and Horseman 1999; Judd et al. 2002).

Methane migration is an important process for two reasons:

1. Methane fluxes in the seabed and into the atmosphere are significant in terms of the global carbon budget because methane is a greenhouse gas (Judd et al. 2002). Hovland et al. (1993) concluded that natural gas seeps on continental shelves account for 3–9% of total global methane emissions.
2. Methane migration has a potential instability effect on slopes. Increasing pore pressure due to free gas accumulation in sediment pore spaces decreases the effective stress and shear strength of the sediments and can cause slope failures (e.g., Prior and Coleman 1984; Hovland and Judd 1988; Yun et al. 1999).

Migration and expulsion of shallow gas can create depressions, such as pockmarks on the seafloor, which are generally related to gas and/or fluid discharge in near-surface sediments (Hovland and Judd 1988). Pockmarks were first discovered in the continental shelf of Nova Scotia, Canada (King and MacLean 1970). They are known to be widely distributed, from coastal areas to deepwater environments, such as in Belfast Bay (Kelley et al. 1994), the Norwegian Trench (Hovland 1981), the Bering Sea (Nelson et al. 1979), the Gulf of Cadiz (Baraza and Ercilla 1996), the continental slope of California (Yun et al. 1999), and in some lakes (Pickrill

G. Çifçi · M. Ergün
Institute of Marine Sciences and Technology, Dokuz Eylül
University, Bakü Street, 35340 Inciralti, Izmir, Turkey

D. Dondurur (✉)
Department of Geophysics, Faculty of Engineering, Dokuz Eylül
University, Kaynaklar Campus, 35160 Buca, Izmir, Turkey
Fax: +90-232-4538366

1993). Pockmarks are typically circular or elongated hollows in shape and their diameters vary from a few meters to a few tens of meters. The depths of pockmarks also vary, from <1 m to tens of meters (Hovland and Judd 1988). Giant pockmark craters up to several hundreds of meters in width and 200 m in depth have also been reported (e.g., Solheim and Elverhoi 1993; Cole et al. 2000).

The purpose of this study is to investigate and discuss the deep and shallow structures of pockmarks in the Yesilirmak River Fan of the Eastern Black Sea Turkish shelf. We integrate high-resolution seismic, MAK-1 deep-towed side-scan sonar, 5-kHz sub-bottom profiler and SIMRAD multi-beam echo-sounder bathymetric data to characterize the structures of the pockmarks. The probable origin and the mechanisms affecting the activation/reactivation of the pockmarks are also discussed.

Tectonic setting

The Black Sea is a large marginal sea located within the Alpine orogenic belt, surrounded by compressive tectonic belts, the Pontides orogeny in the south, Caucasus in the northeast and Crimean Range in the north (Fig. 1). It is located on the western flank of the active Arabia–Eurasia collision and north of the North Anatolian Fault (NAF) that permits the tectonic escape of Anatolia (Rangin et al. 2002). It was considered to be the Late Mesozoic–Early Cenozoic marginal back-arc basin of the northward-subducting Tethys Ocean (Spadini et al. 1996; Robinson et al. 1996; Kazmin et al. 2000). The Black Sea comprised two major extensional basins, the western and the eastern Black Sea sub-basins, and was separated by a complex NW–SE-trending continental Mid-Black Sea Ridge (Robinson et al. 1996), which was subdivided into two parts: the Andrussov Ridge in the north and the Archangelsky Ridge in the south (Fig. 1).

The Eastern Black Sea basin has been undergoing about 12 km of subsidence since the early Tertiary (Finetti et al. 1988). This area was dominated by major extensional faults, which have generated half-graben structures. The Archangelsky and Shatsky ridges represent regionally uplifted footwall blocks to major extensional faults that form the southern and northern continental slopes of the region. However, the southern side of the basin was affected by the reactivation of extensional faults and the development of new reverse faults at the end of the Eocene (Meredith and Egan 2002).

The study area is located in the Yesilirmak River delta on the Turkish shelf of the Eastern Black Sea, over the Sinop Basin towards the Archangelsky Ridge (Fig. 1). The shelf extends northwards down to the continental slope, and the shelf break is located at about 300-m water depth. Throughout the region, the seabed was underlain by a thick accumulation of

unconsolidated, fine-grained sediments deposited in the Sinop Basin between the Archangelsky Ridge and the Turkish margin. The Sinop Basin separates the Archangelsky Ridge and the Turkish mainland and has been affected by the late Miocene normal faults along the Turkish margin and the Archangelsky Ridge (Rangin et al. 2002). The overall compressional deformation of the Sinop Basin was superimposed onto the footwall block forming the Archangelsky Ridge. The geometry of the Sinop Basin was interpreted as a foreland basin. The Archangelsky Ridge shows no deposition from the late Eocene to recent times. Further south, the shelf was flanked by the East Pontic Mountains where intensive submarine volcanic activity took place.

The seismicity of the study area is controlled mainly by the active strike-slip North Anatolian Fault (Fig. 1). The age of the fault is early Pliocene (4–5 Ma) and the total offset range is 72 to 125 km (Barka et al. 2000). Based on GPS data, slip rate is 10 to 20 mm/year along the NAF (Tari et al. 2000). The directly related deformation can be easily seen in the Central Pontides, north of the NAF, and in the Sinop area, south of the Archangelsky Ridge (Görür and Tüysüz 1997).

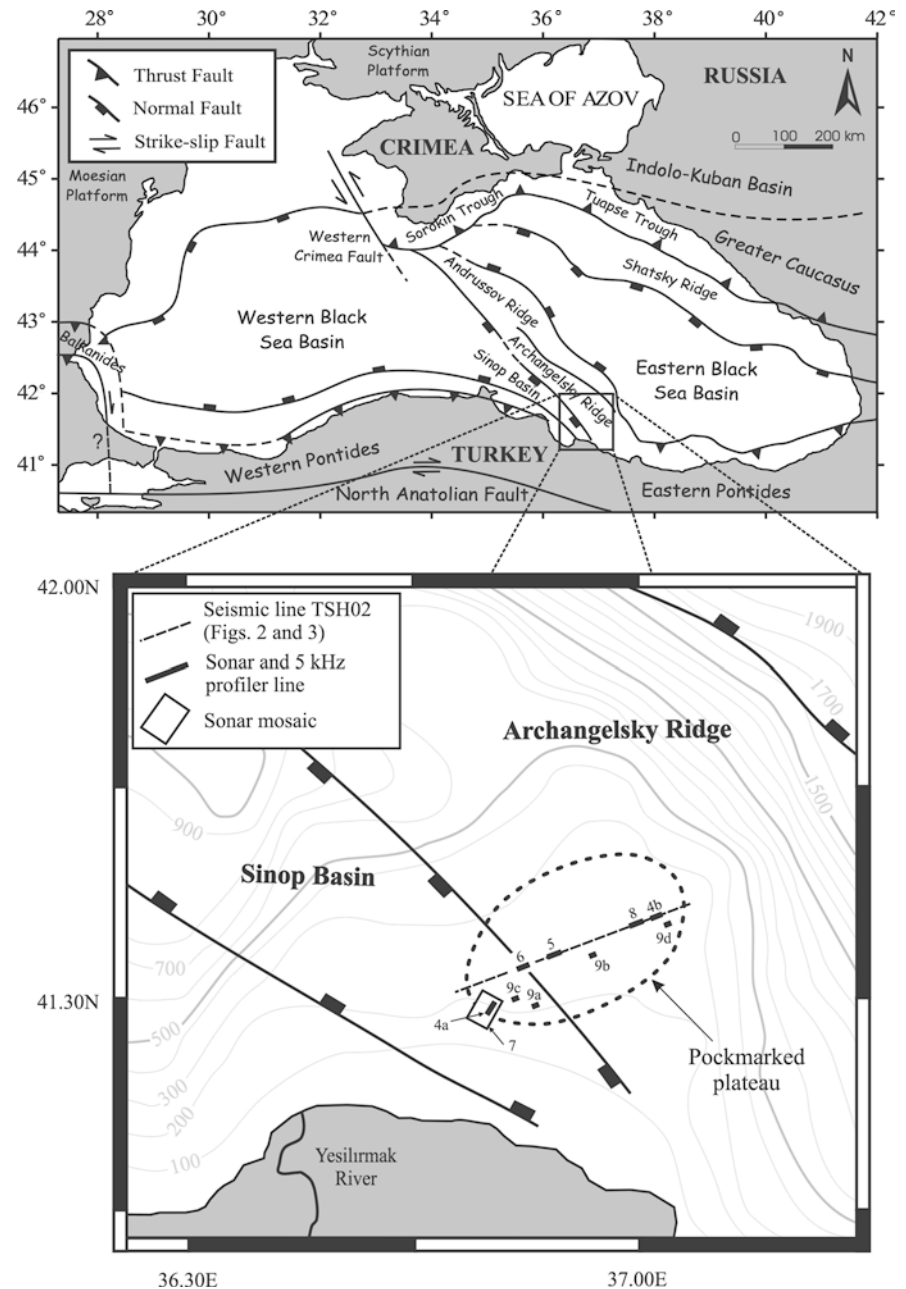
Pockmarks in the study area

The geological setting of the area promotes the formation and migration of gas and overpressured fluid. Large quantities of organic matter supplied by the Yesilirmak River can contribute to excessive amounts of microbial gas (mostly methane) production, associated with pockmark formations and acoustic blanking (Ergün et al. 2002; Çifçi et al. 2002). The overlying plateau of the Archangelsky Ridge (Fig. 1) is marked by numerous pockmarks, appearing as circular and elongated depressions. The pockmark zone is located at water depths of 180–300 m and is an elongated area about 25×7 km in SW–NE direction in the Yesilirmak River delta (Fig. 1). Towards the northeastern margin of the plateau, the pockmarks become more elongated and tend to follow a linear trend. The direction of these linear pockmark trends is sub-parallel to the underlying Archangelsky Ridge axis in E–SE/W–NW direction. The pockmarks are often associated with subsidence structures and slumping of the sediments towards the center.

Deep structure of the pockmarks

A high-resolution airgun seismic line, TSH02 (Figs. 2 and 3), was processed to image the deeper stratigraphic structure of the pockmarked area. The seismic data were collected using a 24-channel recorder with a sampling rate of 0.25 ms and a filter range of 8–1,000 Hz. Shot and group intervals were 3.12 m, with a maximum fold of 12. Following the preprocessing, wave equation

Fig. 1 Simplified tectonic map showing major tectonic elements of the Black Sea (after Robinson et al. 1996; Kazmin et al. 2000). Close-up shows the study area, seismic line TSH02 (*dashed*) and data locations used in the text, together with the limits of the pockmark area (*dotted area*). Numbers next to the data locations represent the corresponding figure numbers. Bathymetric contour interval is 100 m



migration was applied and the data were filtered with an 8–300 Hz band-pass filter.

Figure 2 shows parallel thin sedimentary layers affected by numerous small-offset, nearly vertical growth faults in the TSH02 seismic line in the deeper section of the sedimentary strata in the SW part of the pockmarked area. These faults can be seen in two-way travel times (TWTT) of 450 down to 850 ms. When the location of the growth fault system in Fig. 2 is compared with the close-up of the tectonic map given in Fig. 1, it can be recognized that the locations of the shallow growth faults completely correspond to the southern flank of the Archangelsky Ridge where it is widely affected by extensional normal fault systems. Therefore,

these faults are interpreted as the shallow extensions of the normal fault systems formed along the southern flank of the Archangelsky Ridge connecting the ridge flank to the Sinop Basin.

Faults can provide active conduits for gas and fluid to migrate to the seabed surface and create a fracture permeability allowing gas and fluid to flow to the surface. Two main sedimentary units, affected by growth faults, were distinguished in the interpreted section as unit A and unit B (Fig. 2). Unit A shows mainly parallel and well-bedded sedimentary sequences whereas unit B has a sub-parallel to chaotic reflection pattern. A strong reflector shallows towards the northeast and separates unit A from unit B. The seismic line also shows buried

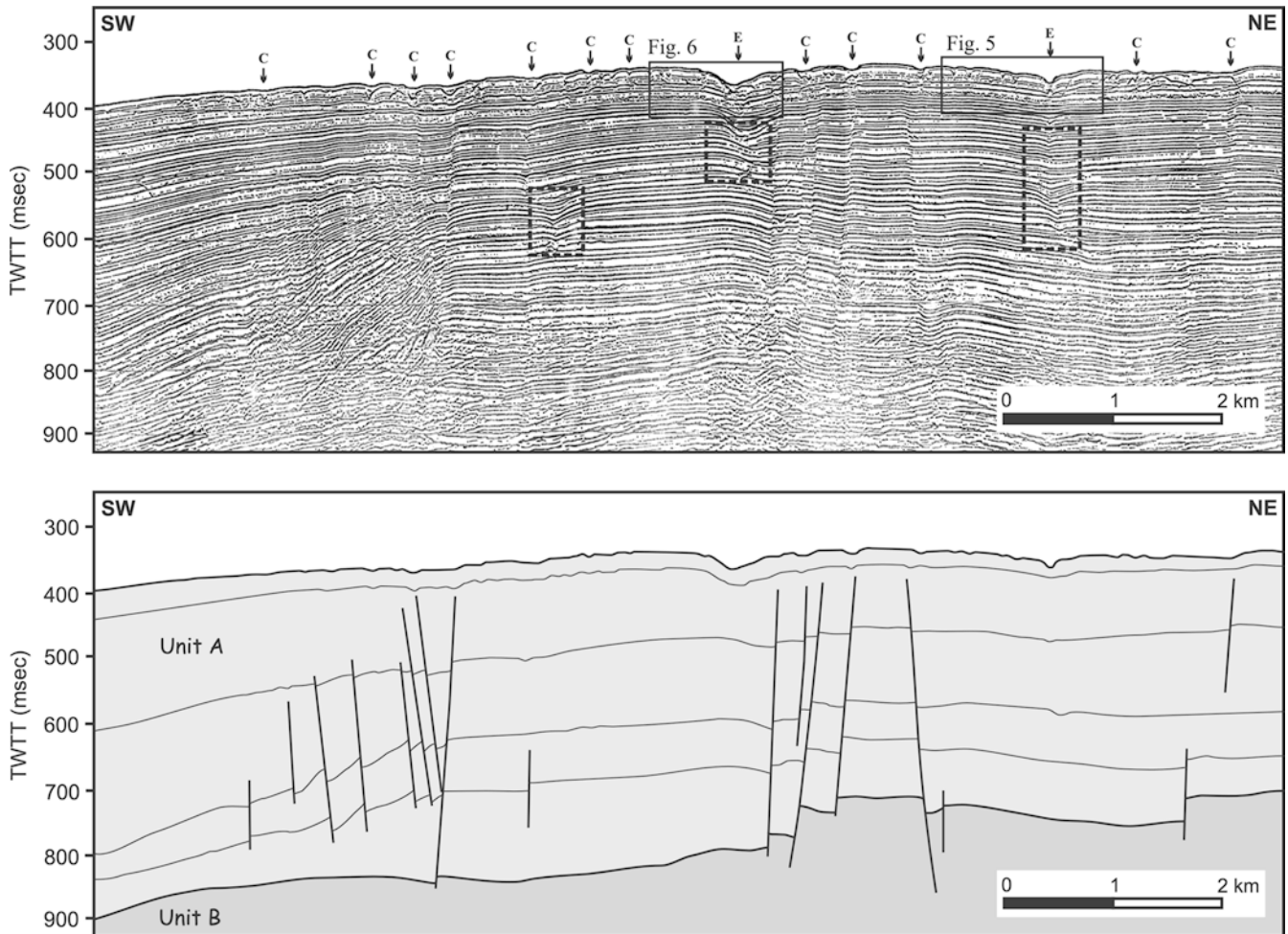


Fig. 2 SW part of seismic line TSH02 and its interpretation (see Fig. 1 for location), showing several small, offset vertical faults and pockmarks on the seafloor (arrows) as well as buried pockmarks in deeper sediments (dashed boxes). Circular and elongated pockmarks are indicated by *C* and *E*, respectively. Insets correspond to 5-kHz sub-bottom profiler sections shown in Figs. 5 and 6

pockmarks (indicated by dashed boxes) in the deep sedimentary strata, and seabed pockmarks as depressions on the seabed (indicated by arrows). The seismic line is perpendicular to the direction of the elongated pockmarks, and thus all the pockmarks are seen as cone-shaped depressions in cross section. The seabed pockmarks can be described as narrow hollows on the seabed.

The NE part of TSH02 is shown in Fig. 3, and a deeper sequence is distinguished as unit C. An erosional truncation (UN in Fig. 3) shallowing towards the NE separates units B and C. The sedimentary layers of unit B overlap this angular unconformity. The growth faults, developed only in unit B, are older than those in Fig. 2 and do not affect unit A. The seismic section shows numerous seabed pockmarks as well as buried pockmarks in the deeper parts of the section. There are more buried pockmarks in the NE part shown in Fig. 3 than those developed in the SW part shown in Fig. 2,

suggesting that there are no well-developed fault systems. The buried pockmarks (indicated by dashed boxes) were generally developed in unit A (Fig. 3) and they form a 'vertically stacked' structure. This interpretation implies that there has been a continuous pockmark development above the same location for long periods of time.

Shallow structure of the pockmarks

In order to investigate the shallow structure of the pockmarks and to get a detailed image of the upper 50 m of the sediments, a 5-kHz sub-bottom profiler and a 100-kHz side-scan sonar (MAK 1 system) were used. Figure 4 shows two examples of sub-bottom profiler data; the first one is from the southern part of the shelf at a water depth of 185 m (Fig. 4a) and the second one is from the northern part with a water depth of 260 m (Fig. 4b). The sedimentary units were observed as parallel layers locally disturbed by the pockmarks. The feeder channels of the pockmarks are clearly visible on the sub-bottom profiler data. These well-developed feeder channels can best be explained by an explosive nature of the pockmarks. The sedimentary sequences in

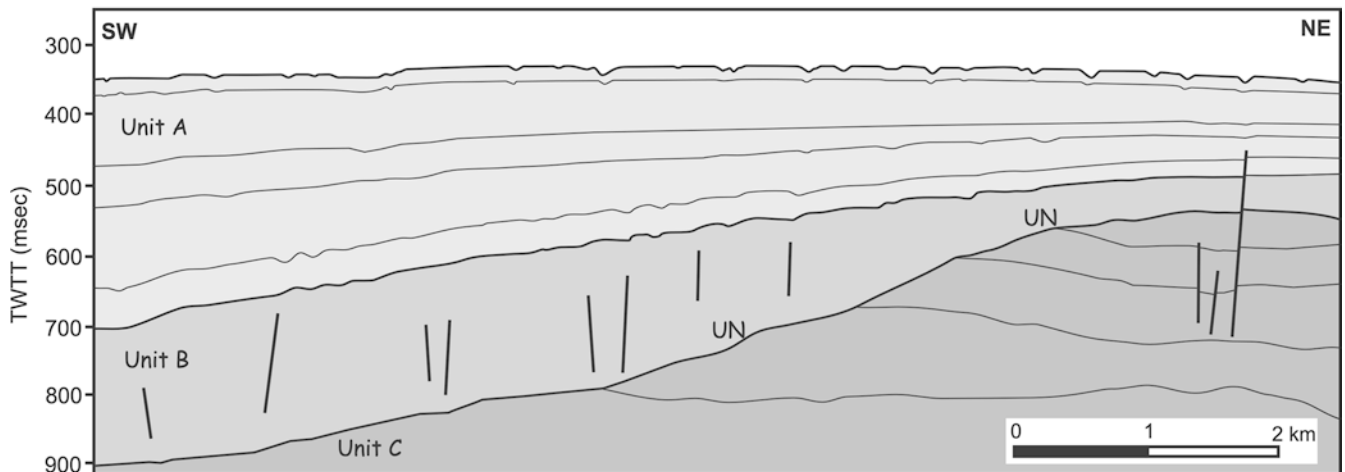
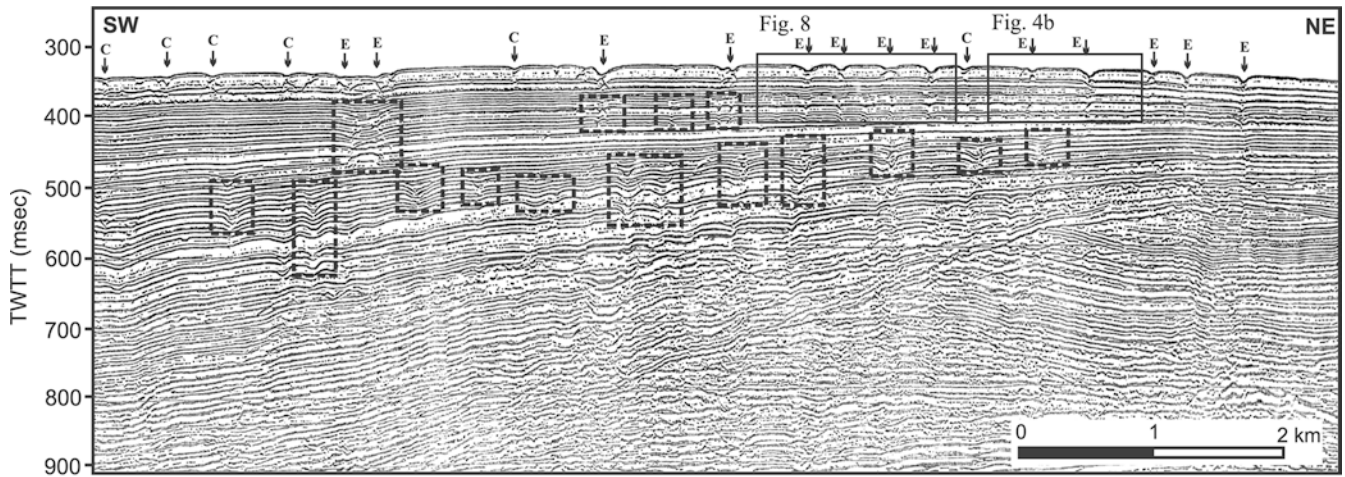


Fig. 3 NE part of seismic line TSH02 and its interpretation (see Fig. 1 for location), showing an unconformity (*UN*) separating units B and C. Other symbols as in Fig. 2. *Insets* correspond to 5-kHz sub-bottom profiler sections shown in Figs. 4b and 8

the vicinity of the feeder channels bend downwards due to collapse after eruption (Fig. 4a). When comparing the shallow structures of the pockmarks for deep and shallow waters, it can be concluded that the deepwater pockmarks are more elongated whereas the shallow-water pockmarks are generally smaller. In addition, the amount of infill for the shallow-water pockmarks is greater than that for the deepwater pockmarks. One

reason for the difference in infill of the craters could be the higher sedimentation closer to shore (southwards), with material transported by the Yesilirmak River. The slope of the seabed is also quite suitable for recent sediments to move towards the north at the nearshore.

As shown in Fig. 5a, b, sonar and multi-beam data indicate that the occurrences of circular patches and elongated structures are pockmarks. The sonar and sub-bottom profiler records also show that pockmarks can merge to form a larger, or elongated, pockmark (Fig. 5b, c). In the SW part of the sub-bottom profiler section (Fig. 5c), gas-filled sediments underlying a strong reflector were observed with acoustic turbidity.

Fig. 4a, b Comparison of shallow-water (a) and deepwater (b) pockmarks. In a, there are two pockmarks at 190- and 200-m water depths (see Figs. 1 and 7 for location), and in b, the pockmarks are at 260-m water depth (see Figs. 1 and 3 for location). Most of the pockmarks in shallower water depths are completely infilled by recent sediments

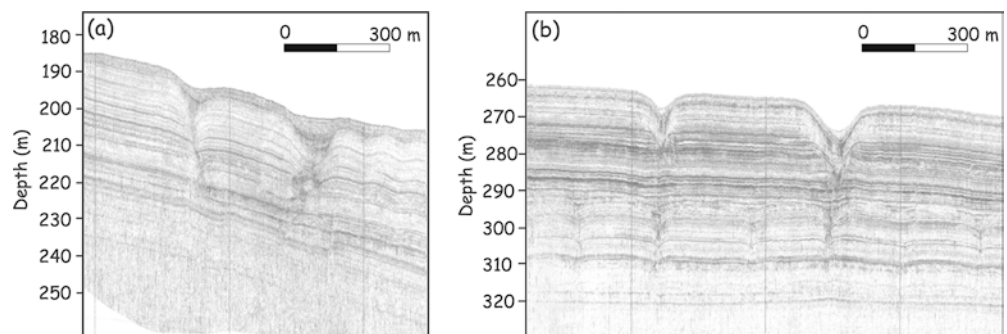


Fig. 5a-c Multi-beam echo-sounder bathymetry (a), side-scan sonar (b), and 5-kHz sub-bottom profiler (c) records (see Figs. 1 and 2 for location). The high-backscattering circular and elongated pockmarks outlined by *dotted lines* on the sonar record in b are observed as depressions on the sub-bottom profiler record in c. It is also observed that the smaller-scale circular pockmarks merge into one, larger elongated pockmark. The SW part of the sub-bottom profiler section also shows gas-filled sediments underlying a highly reflective horizon below 300-m depth. The *dashed rectangle* on the sonar record in b identifies the corresponding area on the multi-beam echo-sounder data in a

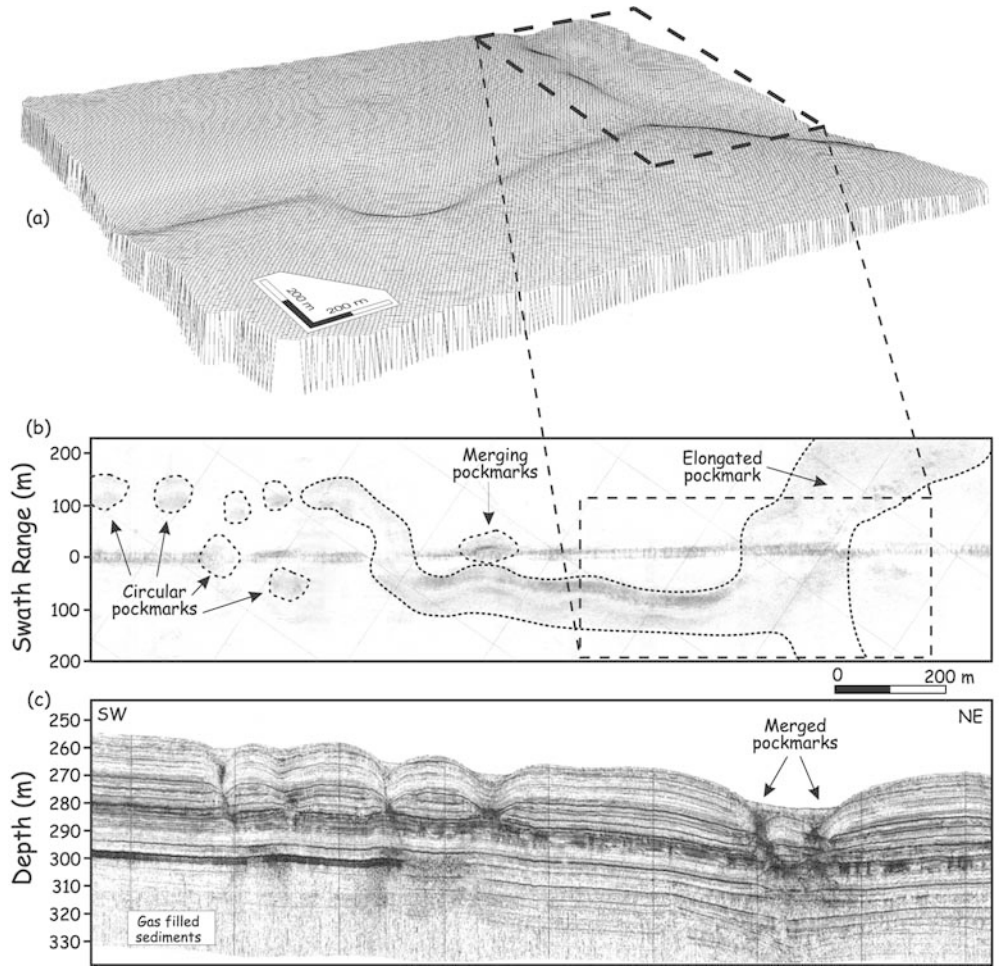


Fig. 6a, b Side-scan sonar (a) and 5-kHz sub-bottom profiler (b) records (see Figs. 1 and 2 for location). The high-backscattering pockmarks are outlined by *dotted lines* on the sonar record in a. Considering the sub-bottom profiler data in b, the elongated pockmark is formed by the merging of two pockmarks with two clearly visible feeder channels. The zone of microfaults observed on the SW part of the profiler section is outlined by a *rectangle*

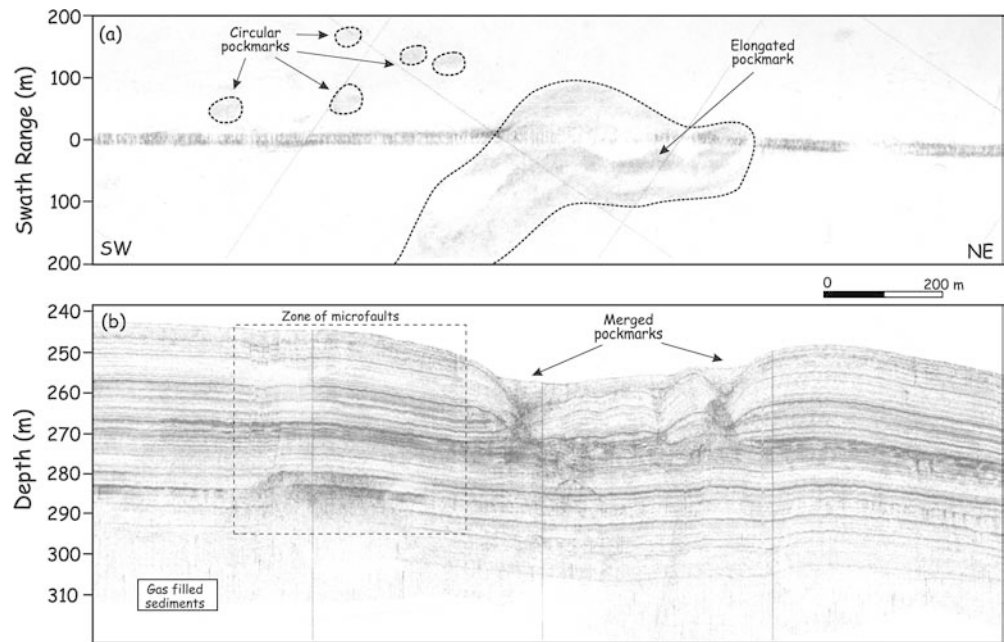


Figure 6 shows another sonar and 5-kHz sub-bottom profiler section with two coalesced pockmarks; each has separate and clearly visible feeder channels, as seen in

Fig. 5 as well. Some microscale faults also exist on the sub-bottom profiler section in Fig. 6b (see Fig. 3 for deeper structures of Figs. 5 and 6).

After the eruption of the pockmarks, coarser material is left inside of the craters due to the winnowing of fine-grained sediments, causing higher backscatter. Therefore, both circular and elongated pockmarks show high backscattering on the sonar data. The high-backscattering circular pockmarks, defined as ‘eyed pockmarks’ by Hovland (1989), are best visible on the sonar data. The sonar mosaic in Fig. 7 shows facies changing from high backscattering in the nearshore sediments to low backscattering in the pockmarked plateau. The facies change, located approximately at the bathymetric contour line of 170 m, determines the transition boundary between the fine-grained clayey sediments in the nearshore, where extensive acoustic gas accumulations and gas masking take place (Çifçi et al. 2002), and the sediments of silty sands where the gas and fluid migrate to the seafloor and generate the pockmarks.

The elongated pockmarks can be seen clearly on the multi-beam echo-sounder bathymetric data. Figure 8 shows a piston core log of 14.7 m, P12, with the multi-beam echo-sounder data from the NE part of the pockmarked plateau, and indicates the occurrence of several parallel pockmarks in elongated form as depressions on the seafloor (see Fig. 3 for deeper structure). The elongated pockmarks are about 200 m wide and can reach a length of 2 km. The distances between the adjacent crater centers of parallel-elongated pockmarks vary from 150 to 250 m. The sub-bottom profiler line was aligned across the elongated structures in the A–B direction and shows strong reflections at a depth of 285 m, overlying gas-filled sediments with acoustic turbidity (Fig. 8b). This strong reflector clearly acts as a cap rock, where gas accumulation was taking place, and is discontinuous in certain zones, where the feeder channels of the seabed and buried pockmarks (indicated as BP) are visible, for example, below the two pockmarks in the SW and NW parts of the section (Fig. 8b). The P12 piston core was sampled inside of the pockmark

crater and mainly soft clays with some shell fragments, particularly in deeper parts, and coccolite laminations in the uppermost parts were recovered. The expansional cracks seen in the core log between 12 and 14.7 m may be related to gas vacuoles.

The circular pockmarks have diameters of 50–120 m whereas the elongated pockmarks have diameters of 150–200 m and can have lengths of 2 km. The depths of the craters for circular and elongated pockmarks are generally not more than 10 m, although depths of more than 25 m were observed, too. The slope angles of the pockmark walls vary between 6 and 12° and the southern flank is generally steeper than the northern flank, forming asymmetric-cone shaped craters, possibly due to downslope turbidity currents.

Discussion

There are several buried pockmarks in vertically stacked form in the deeper sedimentary strata of the pockmarked plateau on the Turkish Shelf. Similar forms of buried pockmarks have also been observed in the Adriatic Sea (Curzi and Veggiani 1985) and the slope of the Gulf of Cadiz (Baraza and Ercilla 1996). This indicates that there is no continuous gas migration to the seabed—rather, the migration of gas is repeated periodically over certain periods of time.

The seabed pockmarks in the area can be classified into four groups that explain the stages of development of both the seabed and buried pockmarks (Fig. 9). In the first stage, the gas accumulation in the uppermost sedimentary sequence under overpressure conditions causes a pockmark expulsion and a depression on the seabed (Fig. 9a). The gas expulsion is mainly active in the first stage, and an acoustically transparent, columnar-shaped zone may still exist just below the pockmark due to the absorption of seismic energy by free gas. The gas

Fig. 7 Part of the sonar mosaic, together with the bathymetric contours in 2-m intervals of the southern part of the pockmarked plateau (see Fig. 1 for location), showing circular and high-backscattering pockmarks as well as a facies change from high-backscattering nearshore sediments to the low-backscattering pockmarked plateau

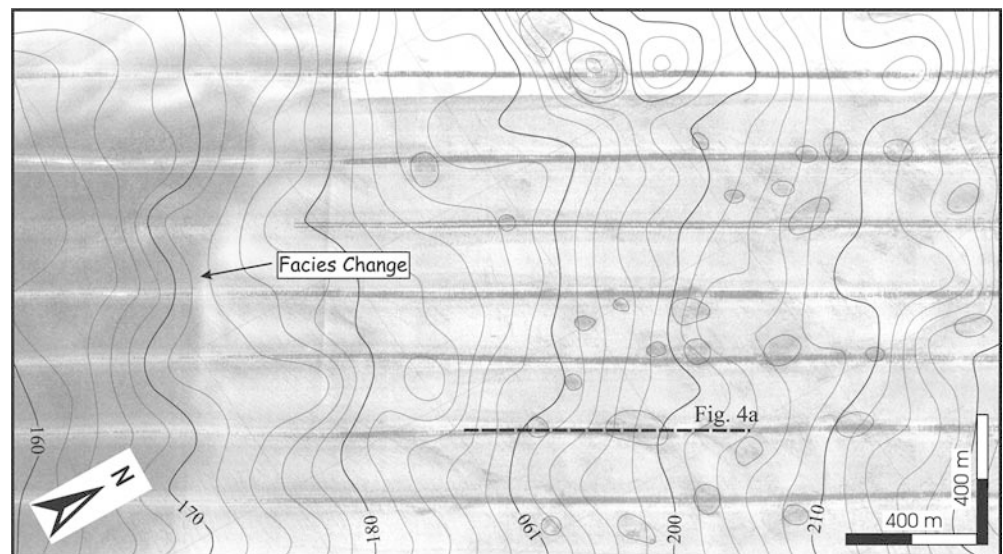
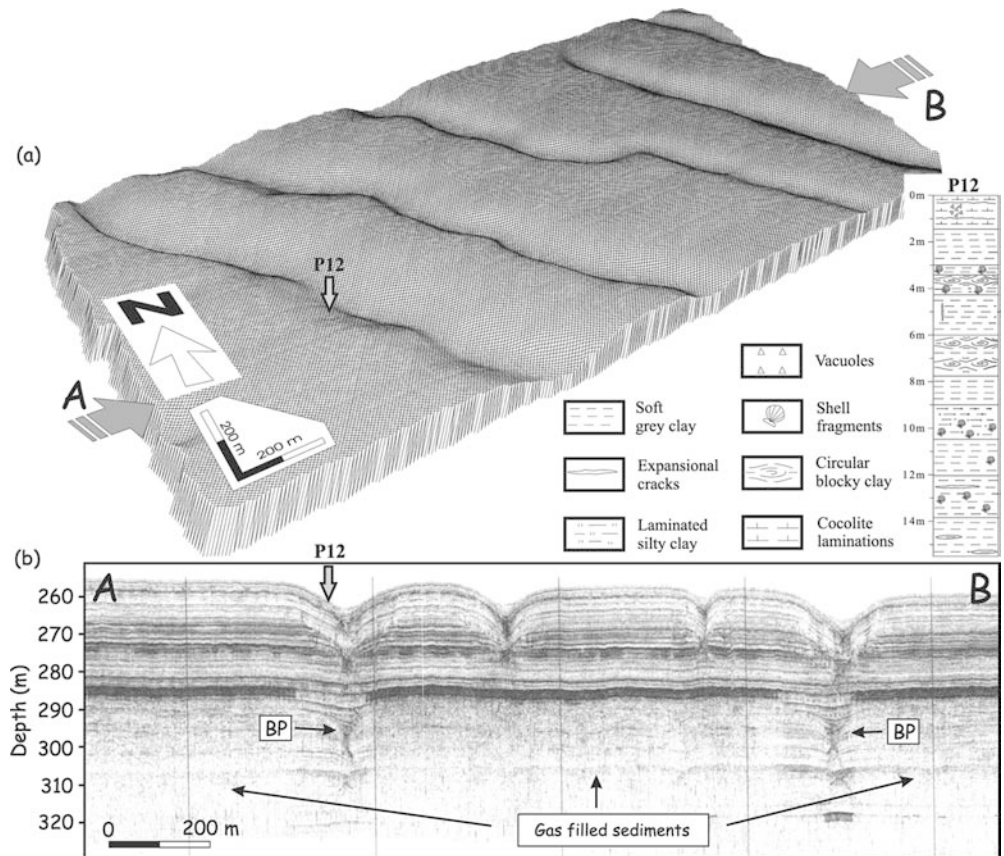


Fig. 8. a Multi-beam bathymetric data from the NE part of the pockmarked plateau, showing a number of parallel elongated pockmarks as depressions on the seabed. The depths of the craters here are not more than 15 m. The elongated pockmarks are approximately 150–200 m wide and 2 km long. **b** Sub-bottom profiler section along *A–B* line on the multi-beam data, perpendicular to the direction of the elongated pockmarks. Buried pockmarks are indicated as *BP*. A strongly reflective horizon, which is discontinuous in place to place below the feeder channels of the pockmarks, overlies gas-filled sediments. The piston core recovered inside of the crater of the pockmark at the southwestern part shows soft clayey sediments and shell fragments as well as coccolite laminations



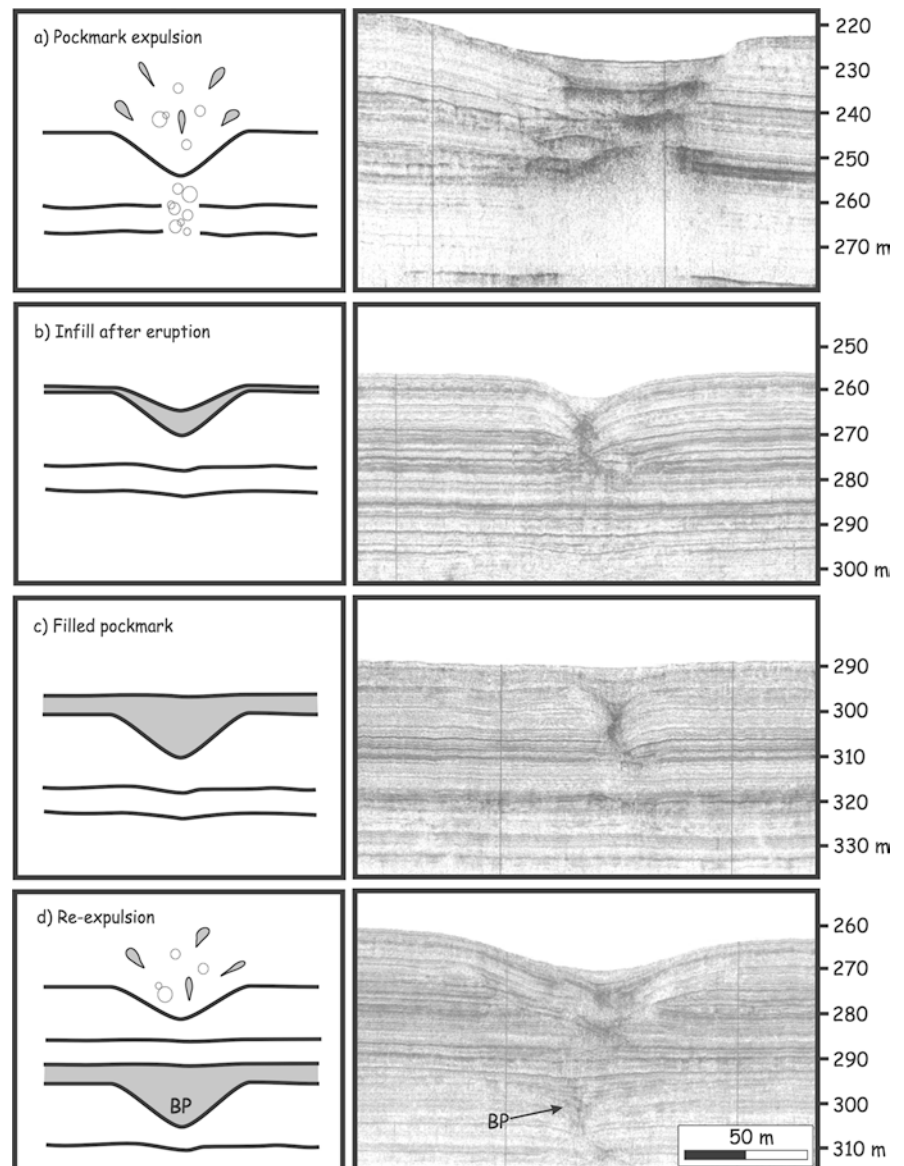
expulsion also prevents recent sediment accumulation in the depression. In the second stage, the expulsion has ceased and recent sediments start filling in the depression formed by the pockmark erupted in the first stage (Fig. 9b). In the third stage, the depression is completely filled by the sediments and the pockmark is buried (Fig. 9c). In the fourth stage, the gas expulsion is reactivated so that a new pockmark is formed on the seabed. The pockmark that erupted previously in the first stage becomes buried (indicated as BP in Fig. 9d). The interruption and reactivation of the gas eruption through the pockmarks continues periodically; in this way, vertically stacked pockmarks are formed.

There could be several reasons for the periodic interruption and reactivation of gas seeping in an area. One reason may be periodical sea-level changes, such as in the Gulf of Cadiz (Baraza and Ercilla 1996) where the expulsion was interrupted during the sea-level low-stand and recent active pockmarks developed during the sea-level high-stand in shallower waters. This explanation fails for the present study area because most of the shallow-water pockmarks were inactive and completely filled by recent sedimentation. An alternative explanation for periodical variations in overpressure conditions is that seismologically driven periodical overpressure generated gas/fluid escape to the seabed. Although the study area was described as a passive margin, the seismically active North Anatolian Fault (NAF; see Fig. 1) could have a significant impact on the regional tectonic

conditions, and could modify the overpressure conditions on the shelf cyclically. The deformation evidence of the Arabian–Anatolian collision is particularly well developed in the Central Pontides, north of the NAF, as in the Sinop region, southern part of the Archangelsky Ridge (Görür and Tüysüz 1997). Rangin et al. (2002) investigated the effect of the NAF on the tectonics at the southern end of the Archangelsky Ridge and in the Sinop Basin. Based on seismic data, they proposed that such fluctuations in stress regime along the NAF have also been evidenced offshore. They also concluded that the opening of the Sinop Basin was the side effect of the incipient motion along the NAF. Therefore, any increase in the stress regime along the NAF near the Black Sea shelf could change the overpressure conditions in the pockmark area, for example, contributing to the pore-pressure increase in the gas-filled sediments and, hence, the expulsion of the accumulated gas via pockmarks.

The development of the elongated pockmarks may be related to recent faulting that provides possible gas escape conduits to the seafloor. If this was the case, these faults need to be traced for hundreds of meters along the elongated pockmarks. However, in the NE part (deeper water) of the area where numerous elongated pockmarks occur, there was no evidence of recent faulting below the pockmarks, since faults in this part did not affect unit A (see Fig. 3). This suggests that the elongated pockmark formations were actually not fault-controlled. We conclude that the smaller-size circular pockmarks coalesce

Fig. 9a–d Schematic illustration (*left column*, not to scale) and corresponding 5-kHz evidence (*right column*, see Fig. 1 for locations) for the evolution of vertically stacked pockmarks. The pockmark structures in the area are classified into four groups explaining the stages of the formation of surface and buried pockmarks. **a** A recently erupted pockmark, **b** start of the infill after eruption, **c** the pockmark completely filled by recent sedimentation, and **d** re-expulsion and formation of a new surface pockmark in the same zone, leaving the former pockmark completely buried (*BP*). The vertical axis in the *right column* is in meters below sea level



late to constitute a single and wider, elongated pockmark. The evidence for this interpretation arises from both the sonar and 5-kHz profiler data. As shown in the profiler data in Figs. 5 and 6, it was evident that the elongated pockmark was formed by the merging of two separate, possibly circular-shaped pockmarks.

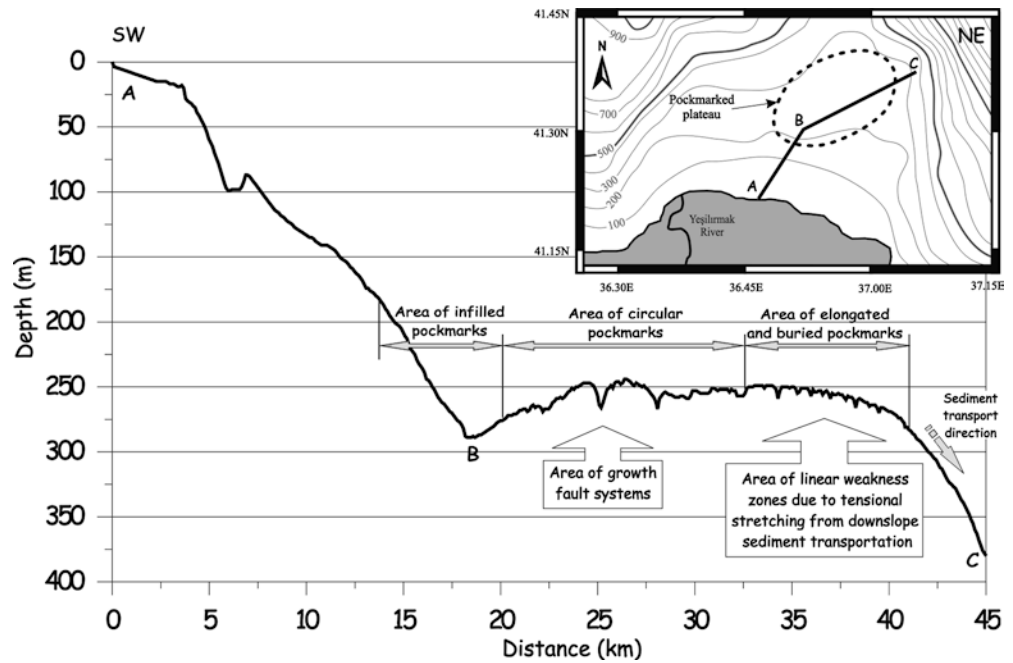
Furthermore, some other mechanisms have also been considered for the formation and merging of the elongated pockmarks. One mechanism is that pockmarks may be eroded by scouring bottom currents (Bøe et al. 1998), and strong sea bottom currents occurring on the shelf edges and continental slopes (e.g., turbidities or density currents) could also create elongated depressions (Hovland et al. 2002).

Turbidity currents are submarine flows of dense mixtures of water and sediment and capable of moving at very high speeds, up to 80 km/h, for distances of tens of kilometers. These can transfer large volumes of sed-

imentary material and are capable of eroding channels on the seafloor. Local current systems possibly exist off the mouth of the Yesilirmak River. It is well known that the river water flows out of the mouth at right angles to the trend of the coastline, and hence it may gradually turn to the east over the shelf break to produce an eddy returning towards the mouth. The flow velocities of these currents are about 20 cm/s in the Yesilirmak Fan (Ergün et al. 2001), and they may have acted as a connector of separate circular pockmarks by removing the recent sediments between the two adjacent pockmarks.

Another mechanism is linked to the increased number of elongated pockmarks towards the shelf break in the NE part of the study area. The elongated pockmarks could be formed by downslope tensional stretching, which may cause linear weakness zones near the upper slope where a sudden increase in slope angle occurs. Ergün et al. (2001) reported that several slump and slide

Fig. 10 Bathymetric cross section from the shore area to the shelf break (e.g., 300-m water depth), together with the location map. The pockmark depressions are clearly observed on the seafloor bathymetry. The pockmark plateau shows three main seabed pockmark provinces, as infilled, circular and elongated as well as buried pockmarks deep in the sedimentary strata



features were formed on the slope and caused a downslope stretching behind the shelf break, located approximately at a depth of 300 m. The stretching may cause some linear weakness zones where the accumulated gas was easily released to the seafloor, allowing the elongated pockmarks to develop. That the directions of the elongated pockmarks are NW to SE (sub-parallel to the bathymetric contour lines) supports this interpretation because the linear weakness zones originating from downslope stretching should be perpendicular to the slope direction, meaning parallel to the shelf break bathymetric contour (300-m contour in Fig. 1). This interpretation is illustrated on a bathymetric cross section with the location map in Fig. 10. Figure 10 also shows the formation provinces of the three main seabed pockmark types—infilled, circular and elongated as well as buried pockmarks. The infilled pockmarks were formed towards the nearshore area, starting at a depth of 180 m, where large amounts of recent sediments filled the craters completely. The slope of the area of infilled pockmarks is quite suitable for recent sediment transportation from the Yesilirmak River (Fig. 10). The pockmark plateau can be subdivided into two parts: as shown in Fig. 10, the southwestern part was affected by deep vertical fault systems, and the seabed pockmarks are generally circular in shape, whereas the northeastern part can be described as the region of elongated seabed pockmarks and vertically stacked, deep buried pockmarks.

Gas in marine sediments is either microbial or thermogenic in origin. In general, it is not possible to determine the origin of the gas in subsurface sediments—either biogenic or thermogenic—just by using acoustic seismic data. However, it may be possible to suggest the existence of gas in the sediments, and seismic

data could provide certain clues about the geological conditions for the evaluation of the gas source.

Large quantities of organic matter transported by the Yesilirmak River produce large amounts of microbial gas resulting in acoustic blanking effects (Ergün et al. 2002; see also Figs. 5 and 8). Figure 9d explains how microbial gas generation could play an important role in forming the pockmarks. As shown in Fig. 9d, a pockmark was buried at about 300 m and was overlaid by undisturbed parallel sedimentary layers. A younger pockmark was also present and indicated a reactivation at the seafloor. The existence of parallel and undisturbed sedimentary layers between these two pockmarks showed that the gas forming in the younger pockmark was produced above these parallel layers. Otherwise, these layers would be disturbed because of the eruption. Therefore, it is concluded that the origin of gas forming in the pockmark was microbial.

Conclusions

The Eastern Black Sea Turkish shelf has been affected by numerous seabed and buried pockmarks in circular and elongated forms. The integration of acoustic methods allowed us to evaluate both deep and shallow structures of the pockmarks in the area. The pockmarks were formed in explosive nature in tectonically relaxed zones in the pockmark plateau, located between the bathymetric contours of 180 and 300 m. The circular pockmarks varied strongly in size, 50 to 120 m, but the elongated pockmarks were much wider, 200 to 250 m, and could be traced about 2 to 3 km. It is concluded that these wider elongated pockmarks were formed by merging of the smaller-sized circular pockmarks. Strong

bottom currents and downslope tensional stretching may cause linear weak zones near the upper slope, playing an important role in the merging of the pockmarks. Both types of pockmarks were observed as high-backscattering depressions on the sonar and the profiler data.

The existence of numerous buried pockmarks in deeper sediments of the pockmarked plateau indicates that gas migration to the seabed was not continuous but repeated periodically over long time periods. We conclude that the reason for the periodical interruption and reactivation of the gas seeping in the area was the seismologically driven, periodical variation in overpressure conditions. The seismologically active North Anatolian Fault has had a significant effect on the tectonic and overpressure conditions in the area, and could modify the overpressure conditions of the shelf cyclically.

The slope angles of the pockmark walls varied between 6 and 12° and the southern flank was generally steeper because of the downslope turbidity currents that form asymmetric, cone-shaped craters. The sidewalls of pockmarks, particularly the fresh ones, may be steep and unstable. Therefore, slope stability was influenced by these sediments, and should be taken into account for nearshore and offshore construction studies.

Acknowledgements We sincerely thank Dr. Casey Moore, Dr. Lars Zuesdorff and Dr. Janet Yun for their helpful and constructive comments in reviewing of the manuscript. We also would like to thank Dr. Zafer Y. Öner for his valuable comments on an earlier version of this paper. This research was supported by a grant (project code 100Y078) from The Scientific and Technical Research Council of Turkey (TUBITAK) and by Dokuz Eylül University Research Foundation grants (project codes 02.KB.FEN.064 and 02.KB.FEN.025).

References

- Acosta J (1984) Occurrence of acoustic masking in sediments in two areas of the continental shelf of Spain: Ria de Muros (NW) and Gulf of Cadiz (SW). *Mar Geol* 58:427–434
- Baraza J, Ercilla G (1996) Gas-charged sediments and large pockmark-like features on the Gulf of Cadiz slope (SW Spain). *Mar Petrol Geol* 13:253–261
- Barka A, Akyüz HS, Cohen HA, Watchorn F (2000) Tectonic evolution of the Nixsar and Tasova–Erbaa pull-apart basins, North Anatolian Fault Zone: their significance for the motion of the Anatolian block. *Tectonophysics* 322:243–264
- Bøe R, Rise L, Ottesen D (1998) Elongate depressions on the southern slope of the Norwegian Trench (Skagerrak): morphology and evolution. *Mar Geol* 146:191–203
- Çiğçi G, Dondurur D, Ergün M (2002) Sonar and high resolution seismic studies in the Eastern Black Sea. *Turkish J Earth Sci* 11:61–81
- Cole D, Stewart SA, Cartwright JA (2000) Giant irregular pockmark craters in the Palaeogene of the Outer Moray Firth Basin, UK North Sea. *Mar Petrol Geol* 17:563–577
- Curzi PV, Veggiani A (1985) I pockmarks nel mare Adriatico centrale. *Acta Nat Ateneo Parmense* 21:9–90
- Ergün M, Çiğçi G, Dondurur D (2001) High resolution seismic and sonar characteristics of the Eastern Black Sea Turkish continental slope. In: 36th CIESM Congr, Monaco. *Rapp Comm Int Mer Méditerranée*, 36
- Ergün M, Dondurur D, Çiğçi G (2002) Acoustic evidence for shallow gas accumulations in the sediments of the eastern Black Sea. *Terra Nova* 14:313–320
- Fader GBJ (1991) Gas-related sedimentary features from the eastern Canadian continental shelf. *Cont Shelf Res* 11:1123–1153
- Finetti IR, Bricchi G, DelBen A, Pipan M, Xuan Z (1988) Geophysical study of the Black Sea. In: Finetti IR (ed) *Monograph on the Black Sea*. *Boll Geophys Teor Appl Trieste Italy* 30:197–324
- Garcia-Garcia A, Vilas F, Garcia-Gill S (1999) A seeping sea-floor in a Ria environment: Ria de Vigo (NW Spain). *Environ Geol* 38:296–300
- Görür N, Tüysüz O (1997) Petroleum geology of the southern continental margin of the Black Sea. In: Robinson AG (ed) *Regional and petroleum geology of the Black Sea and surrounding region*. *AAPG Mem*, pp 241–254
- Harrington JF, Horseman ST (1999) Gas transport properties of clays and mudrocks. In: Aplin AC, Fleet AJ, Macquaker JHS (eds) *Muds, mudstones: physical fluid properties*. *Geol Soc Lond Spec Publ* 158:107–124
- Hart BS, Hamilton TS (1993) High resolution acoustic mapping of shallow gas in unconsolidated sediments beneath the Strait of Georgia, British Columbia. *Geo-Mar Lett* 13:49–55
- Hovland M (1981) Characteristics of pockmarks in the Norwegian Trench. *Mar Geol* 39:103–117
- Hovland M (1989) Modern analogues to Middle Ordovician sedimentary mounds and washout depressions. *J Sediment Petrol* 59:585–589
- Hovland M, Curzi P (1989) Gas seepage and assumed mud diapirism in the Italian Central Adriatic Sea. *Mar Petrol Geol* 6:161–169
- Hovland M, Judd AG (1988) Seabed pockmarks and seepages, impact on geology, biology and the marine environment. Graham and Trotman, London
- Hovland M, Judd AG, Burke RA (1993) The global production of methane from shallow submarine sources. *Chemosphere* 26:559–578
- Hovland M, Gardner JV, Judd AG (2002) The significance of pockmarks to understanding fluid flow processes and geohazards. *Geofluids* 2:127–136
- Judd AG, Sim R (1998) Shallow gas migration mechanisms in deep water sediments. In: Ardu DA, Hobbs R, Horsnell M, Jardine R, Long D, Sommerville J (eds) *Offshore site investigation and foundation behaviour: new frontiers*. *Soc Underwater Technol Lond*, pp 163–174
- Judd AG, Hovland M, Dimitrov LI, Garcia-Gill S, Jukes V (2002) The geological methane budget at continental margins and its influence on climate change. *Geofluids* 2:109–126
- Kazmin VG, Schreider AA, Bulychev AA (2000) Early stages of evolution of the Black Sea. In: Bozkurt E, Winchester JA, Piper JDA (eds) *Tectonics and magmatism in Turkey and the surrounding area*. *Geol Soc Lond Spec Publ* 173:235–249
- Kelley JT, Dickson SM, Belknap DF, Barnhardt WA, Henderson M (1994) Giant sea-bed pockmarks: evidence for gas escape from Belfast Bay. *Mar Geol* 22:59–62
- King LH, MacLean B (1970) Pockmarks on the Scotian Shelf. *Geol Soc Am Bull* 81:3141–3148
- Meredith DJ, Egan SS (2002) The geological and geodynamic evolution of the eastern Black Sea basin: insights from 2-D and 3-D tectonic modeling. *Tectonophysics* 350:157–179
- Milliman JD, Butenko J (1985) Geohazards in the Yellow Sea and East China Sea. In: *Proc Offshore Technology Conf 1985*, Houston, Texas, Pap 4965
- Moore JC, Brown KM, Horath M, Cochrane G, MacKay M, Moore G (1991) Plumbing accretionary prisms. In: Tarney J, Pickering KT, Knipe RJ, Dewey JF (eds) *The behavior and influence of fluids in subduction zones*. *R Soc Lond*, pp 49–62
- Nelson H, Tor DR, Sandstrom MW, Kvenvolden KA (1979) Modern biogenic gas-related craters (sea-floor ‘pockmarks’) on the Bering Shelf, Alaska. *Geol Soc Am Bull* 90:1144–1152

- Orange DL, Yun JW, Maher N, Barry J, Greene G (2002) Tracking California seafloor seeps with bathymetry, backscatter and ROVs. *Cont Shelf Res* 22:2273–2290
- Pickrill RA (1993) Shallow seismic stratigraphy and pockmarks of a hydrothermally influenced lake, Lake Rotoiti, New Zealand. *Sedimentology* 40:813–828
- Prior DB, Coleman JB (1984) Submarine slope instability. In: Brunson D, Prior DB (eds) *Slope instability*. Wiley, New York, pp 419–455
- Rangin C, Bader AG, Pascal G, Ecevitoglu B, Görür N (2002) Deep structure of the Mid Black Sea High (offshore Turkey) imaged by multi-channel seismic survey (BLACKSIS Cruise). *Mar Geol* 182:265–278
- Robinson AG, Rudat JH, Banks CJ, Wiles RLF (1996). Petroleum geology of the Black Sea. *Mar Petrol Geol* 13:195–223
- Schüller F (1952) Untersuchungen über die Mächtigkeit von Schlickschichten mit Hilfe des Echographen. *Dt Hydrogr Z* 5:220–231
- Solheim A, Elverhoi A (1993) Gas-related sea floor craters in the Barents Sea. *Geo-Mar Lett* 13:235–243
- Spadini G, Robinson AG, Cloetingh SAPL (1996) Western versus eastern Black Sea tectonic evolution: pre-rift lithospheric controls on basin formation. *Tectonophysics* 266:139–154
- Tarı E, Sahin M, Barka A, Reilinger R, King RW, McClusky S, Prilepin M (2000) Active tectonics of the Black Sea with GPS. *Earth Planets Space* 52:747–751
- Yun JW, Orange DL, Field ME (1999) Subsurface gas offshore of northern California and its link to submarine geomorphology. *Mar Geol* 154:357–368